Biogeochemistry
DOI 10.1007/s10533-016-0230-8

Intermediate-scale community-level flux of CO_2 and CH_4 in a Minnesota peatland: putting the SPRUCE project in a global context

P. J. Hanson · A. L. Gill · X. Xu · J. R. Phillips · D. J. Weston · R. K. Kolka · J. S. Riggs · L. A. Hook

Received: 28 March 2016 / Accepted: 22 July 2016
© The Author(s) 2016. This article is published with open access at Springerlink.com

Abstract Peatland measurements of CO_2 and CH_4 flux were obtained at scales appropriate to the in situ biological community below the tree layer to demonstrate representativeness of the spruce and peatland responses under climatic and environmental change (SPRUCE) experiment. Surface flux measurements were made using dual open-path analyzers over an area of 1.13 m^2 in daylight and dark conditions along with associated peat temperatures, water table height, hummock moisture, atmospheric pressure and incident radiation data. Observations from August 2011 through December 2014 demonstrated seasonal trends correlated with temperature as the dominant apparent driving variable. The S1-Bog for the SPRUCE study was found to be representative of temperate peatlands in terms of CO_2 and CH_4 flux. Maximum net CO_2 flux in midsummer showed similar rates of C uptake and loss: daytime surface uptake was −5 to −6 μmol m^{-2} s^{-1} and dark period loss rates were 4–5 μmol m^{-2} s^{-1} (positive values are carbon lost to the atmosphere). Maximum midsummer CH_4-C flux ranged from 0.4 to 0.5 μmol m^{-2} s^{-1} and was a factor of 10 lower than dark CO_2–C efflux rates. Midwinter conditions produced near-zero flux for both CO_2 and CH_4 with frozen surfaces. Integrating temperature-dependent models across annual periods showed dark CO_2–C and CH_4–C flux to be 894 ± 34 and 16 ± 2 gC m^{-2} y^{-1}, respectively. Net ecosystem exchange of carbon from the shrub-forb-*Sphagnum*-microbial community (excluding tree contributions) ranged from −3.1 gCO_2–C m^{-2} y^{-1} in 2013, to C

Responsible Editor: Melanie A. Vile

Notice: This manuscript has been authored by UT-Battelle, LLC under Contract No. DE-AC05-00OR22725 with the U.S. Department of Energy. The United States Government retains and the publisher, by accepting the article for publication, acknowledges that the United States Government retains a non-exclusive, paid-up, irrevocable, world-wide license to publish or reproduce the published form of this manuscript, or allow others to do so, for United States Government purposes. The Department of Energy will provide public access to these results of federally sponsored research in accordance with the DOE Public Access Plan (http://www.energy.gov/downloads/doe-public-access-plan).

Electronic supplementary material The online version of this article (doi:10.1007/s10533-016-0230-8) contains supplementary material, which is available to authorized users.

P. J. Hanson (✉) · J. R. Phillips · D. J. Weston · J. S. Riggs · L. A. Hook
Oak Ridge National Laboratory, Climate Change Science Institute and Environmental Sciences Division, Oak Ridge, TN 37831-6301, USA
e-mail: hansonpj@ornl.gov

A. L. Gill
Boston University, Boston, MA 02215, USA

X. Xu
San Diego State University, San Diego, CA 92182, USA

Published online: 20 August 2016

losses from 21 to 65 gCO_2–C m^{-2} y^{-1} for the other years.

Keywords Carbon budget · Carbon dioxide · Methane · Peat · *Picea* · *Sphagnum*

Abbreviations

C	carbon
CO_2	carbon dioxide
CH_4	methane
MEF	Marcell Experimental Forest
PAR	photosynthetically active radiation

Introduction

Peatlands currently represent a major global carbon sink sensitive to climate change, although the effect of future warming on the fate of stored carbon (C) is largely unknown (Gorham 1991; Bubier and Moore 1994; Tarnocai and Stolbovoy 2006; Heijmans et al. 2008). Characterizing peatland uptake of atmospheric carbon dioxide (CO_2) and loss of stored C (as CO_2 and methane [CH_4]) is notoriously difficult due to the spatial and temporal variability of gas fluxes, the methodological challenges of measuring surface fluxes, the multi-faceted interactions between many environmental drivers that influence trace gas emission (e.g., temperature, water saturation, peat oxygen content, substrate availability), and the remote nature of many high latitude peatlands. Current projections of future climate conditions suggest that temperate peatlands may experience 4–6 °C warming by the end of the 21st century (IPCC 2013). Therefore, placing observed rates of CO_2 and CH_4 release in the context of future warming represents an additional challenge as predicted levels of sustained warming go beyond the range of historical climate variation experienced by extant peatlands.

Mechanistic models are powerful tools that can be leveraged to project future carbon dynamics in peatlands (Tian et al. 2010; Wania et al. 2010; Riley et al. 2011), but provide a solution only if they can be parameterized and benchmarked with appropriate data. Large-scale, multi-factor global change experiments are an ideal place to generate such empirical, ecosystem-scale data, but typically require relatively small experimental plots that must remain undisturbed throughout the duration of the experiment. Accurately characterizing net ecosystem exchange of carbon (NEE) within manipulation plots is therefore a challenge. The small size precludes ecosystem-scale measurements such as eddy covariance, but adequately distributed small static chambers can be used to capture spatial variation in carbon uptake and loss, especially across heterogeneous peat topography. Peatlands are characterized by an uneven or variable hummock-hollow surface topography that has often, and appropriately, required the measurement and interpretation of surface flux observations at multiple locations representative of this diversity (Belyea and Baird 2006; Lai et al. 2014a). Such measurements benefit from modeling approaches that recognize surface variation details (e.g., Baird et al. 2009; Shi et al. 2015).

Here we use a community-scale collar approach to characterize pretreatment surface fluxes of CO_2 and CH_4 at the spruce and peatland responses under climate and environmental change experiment (SPRUCE: http://www.mnspruce.ornl.gov). In this study we addressed the question: how representative is the SPRUCE peatland in terms of CO_2 and CH_4 flux for known peatlands? We also characterized the spatial heterogeneity of peat surface CO_2 and CH_4 fluxes within the S1-Bog prior to SPRUCE treatment initiation. The measurements provide pretreatment characterizations of the peatland community below tree canopies using an approach that preserves plot integrity over the planned ten-year treatment period. The project employs simultaneous measurements of CO_2 and CH_4 flux using open path instrumentation to provide quantitative data on the gas fluxes from the peatland, and characterizes the seasonal and spatial dynamics and annual contribution to the peatland carbon cycle. These community level observations are complementary to traditional small collar observations of surface CO_2 and CH_4 flux (e.g., Dise et al. 1993; Song et al. 2009, 2012). These measurements represent a viable option for multi-year, community-level measurements within a manipulated ecosystem enclosure when eddy covariance approaches (Olson et al. 2013) cannot be applied.

R. K. Kolka
Forestry Sciences Laboratory, USDA Forest Service, Northern Research Station, Grand Rapids, MN 55744, USA

Methodology

SPRUCE project

The SPRUCE project is an experiment to assess the response of northern peatland ecosystems to increases in temperature and exposures to elevated atmospheric CO_2 concentrations. The experimental work is being conducted in a *Picea mariana* [black spruce]—*Sphagnum* spp. bog in northern Minnesota, 40 km north of Grand Rapids, in the USDA Forest Service Marcell Experimental Forest (MEF). The site is located at the southern margin of the boreal forest in a temperate climate. Experimental work in the 8.1-ha S1-Bog includes a climate change manipulation focusing on the combined responses to multiple levels of warming at ambient or elevated CO_2 levels. SPRUCE evaluates the response of the existing biological communities to a range of warming levels from ambient to +9 °C within large, open-top enclosures (Krassovski et al. 2015; Barbier et al. 2012). Half of the warming treatments are also conducted at eCO_2 (~900 ppm). Both direct and indirect effects of these experimental perturbations will be analyzed to develop and refine models needed for full Earth system analyses.

Site description

All measurements were conducted at the SPRUCE site located on the S1-Bog within the MEF (N47°30.476′; W93°27.162′ and 418 m above mean sea level; Kolka et al. 2011). The climate of the MEF is subhumid continental, with wide and rapid diurnal and seasonal temperature fluctuations (Verry et al. 1988). Over the period from 1961 through 2005 the average annual air temperature was 3.3 °C, with daily mean extremes of −38 and 30 °C, and the average annual precipitation was 768 mm. Mean annual air temperatures have increased about 0.4 °C per decade over the last 40 years (Sebestyen et al. 2011).

The S1-Bog is a weakly ombrotrophic peatland with a perched water table that has little regional groundwater influence. The S1-Bog is dominated by *Picea mariana* (Mill.) B.S.P. (black spruce) with contributions to the forest canopy from *Larix laricina* (Du Roi) K. Koch (larch). The S1-Bog was harvested in strip cuts in 1969 and 1974 to test the effects of seeding on the natural regeneration of *P. mariana*. In its current state the canopy is 5–8 m tall. The peatland soil is the Greenwood series, a Typic Haplohemist (http://www.websoilsurvey.nrcs.usda.gov) with average peat depths to the Wisconsin glacial-age lake bed of 2–3 m (Parsekian et al. 2012), but depths to 11 m are present. Recent surveys of the peat depth, bulk density, and carbon concentrations for the S1-Bog suggest a total C storage pool commonly greater than 200 kgC m^{-2}, with greater than 90 % more than 3000 years old (Karis McFarlane, personal communication).

Below-canopy vegetation within the S1-Bog is composed of a bryophyte layer including *Pleurozium* spp. (feather mosses), *Polytrichum* spp (haircap mosses) and dominated by *Sphagnum* spp. mosses, especially *Sphagnum angustifolium* and *fallax* in hollows and *Sphagnum magellanicum* on drier hummocks. The understory includes a layer of ericaceous shrubs including *Rhododendron groenlandicum* (Oeder) Kron and Judd (Labrador tea), *Chamaedaphne calyculata* (L.) Moench. (leatherleaf) with a minor component of other woody shrubs. The bog also supports a limited number of herbaceous species including: the summer-prevalent *Mianthemum trifolium* (L.) Desf. (three-leaf false Solomon's seal), a variety of sedges (*Carex* spp.) and *Eriophorum spissum* (cotton grass). The belowground peat profile and geochemistry are described in Tfaily et al. (2014).

The flux measurement system

We designed a community-level flux measurement system that uses open path sensors to simultaneously measure CO_2 and CH_4 exchanges in 1.2 m internal diameter chambers. Closed path spectrometers, most often used for small-scale dual measurements of methane and carbon dioxide flux, require a pump to reduce laser cavity pressure, and thus have high power requirements. In contrast, open path sensors do not require such a pump and have a much smaller power draw, which is ideal when infrastructure is limited. While moisture collection and ice crystallization can interfere with open path sensors and require that data be filtered during precipitation events when applied in eddy covariance applications, short term collar-level flux avoid these problems, but reap the benefits of low power draw, lighter instrumentation, and no tubing or analysis delay.

The large 1.2 m diameter chambers incorporate a visually-determined, locally representative sample of the aboveground plant community (excluding widely spaced trees). Ecosystem features encompassed by this method include a hummock-hollow topography covered with *Sphagnum* spp. with ~30 cm of elevation difference, the presence of ericaceous shrubs with a mean height of 30–40 cm, and an ephemeral *Maianthemum trifolium* community occupying the hollow areas. The hummock-hollow spatial pattern from hollow bottoms to hummocks tops repeats at a 0.5–1 m interval in the S1-Bog; our collars cover a complete hummock and hollow topography.

Climate-hardy infrastructure and durable instrumentation were selected to ensure repeated and comparable flux observations over the multi-year study. We used paired open-path sensors to characterize changing H_2O, CO_2 and CH_4 concentrations within a sealed and transparent enclosure space following the concepts for desert plant communities previously described by Arnone and Obrist (2003) to measure flux rates from the intact bog community (Fig. 1). The measurement system using embedded open-path analyzers is considered a community-scale approach to distinguish it from traditional small and static chamber techniques that do not incorporate vertically structured soil and vegetation. However, we do recognize that other peatland static chamber approaches have also used chambers large enough to include the full complement of community vegetation (e.g., Ballantyne et al. 2014).

We constructed flux collars from the top 67 cm of a commercially available linear polyethylene tank (Chem-Tainer Industries, Inc., West Babylon, New York; Part No. TC4842AA-Black). We used a black polyethylene collar to eliminate light penetration, and subsequently painted it white to minimize local temperature changes in the bog surface environment. The collar was embedded 10–20 cm into the surface peat (defined as the hollow height) to achieve an air-tight seal at ground level. At the time of each flux assessment, 10 observations from collar height to

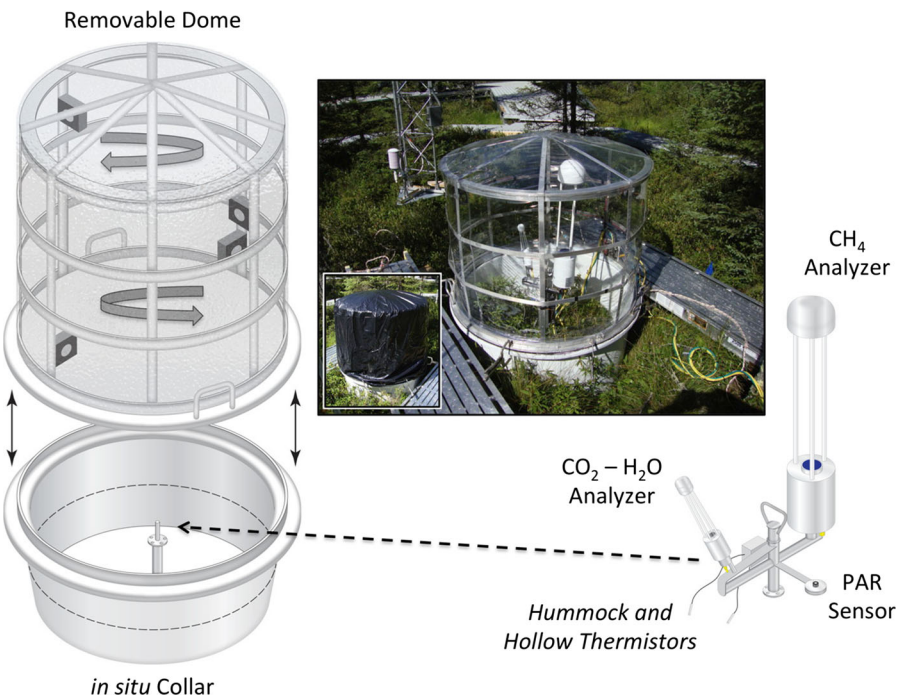

Fig. 1 Diagrams and photographs of the complete CH_4–CO_2–H_2O measurement system installed for observations in the S1-Bog. A permanent in situ collar and instrument stand remain in the peatland. The instrument package and transparent dome are assembled in and over the collar, respectively, for each short term measurement. The *photograph* shows the transparent chamber clamped to the permanent collar with internal instrumentation in place during a typical measurement. The *inset* photograph shows the system enshrouded with a temporary *black plastic cover* for dark or pseudo-nighttime observations. Platforms on either side of the collar and chamber are installed above the shrubs for temporary access during measurements

Sphagnum surface were made across the collar area and averaged to determine the collar volume. Individual collar volumes ranged from 0.45 to 0. 69 m^3 due to between-collar variation in the bog topography.

The transportable and transparent enclosure (removable top in Fig. 1) was constructed of a cylindrical aluminum frame (1.3 m diameter × 1.02 m tall) to be placed above a 1.35 m diameter circular ring formed from 5 cm aluminum angle material. The frame was covered with a transparent polyethylene fitted plastic cover with light transmittance greater than 90 % in the absence of structural shadows. The plastic cover was sealed to the aluminum angle ring with a tension band. Four 12-volt DC fans (Link Depot Model E244875 0.35 A)] were positioned within the transparent enclosure to stir the upper 1.25 m^3 volume, but no fans were added to the collar area to minimize surface boundary layer disturbance. The total enclosed volume during measurements was approximately 1.8 m^3, but varied by collar depending on the surface characteristic of individual plots. Internal volumes were determined from dimensional measurements and geometric calculations. Porosity of the peat surface itself was assumed to lie within a defined boundary layer that did not contribute to the chamber volume calculations.

During measurements, the upper and lower enclosure frames were joined together with a ½ inch thick, closed-cell neoprene foam gasket and tightened with six welding clamps spaced around the circumference of the chamber. All plots were accessed from an interconnected boardwalk system suspended above the surface of the bog to eliminate plot disturbance.

Open-path CO_2 × H_2O (LI-7500A; LiCor Inc., Lincoln, NE) and CH_4 (LI-7700; LiCor Inc. Lincoln, NE) infrared sensors were mounted to a metal carrying device that was placed on a permanent stainless steel post (driven to a depth >2 m) located in the center of each collar (Fig. 1).

The analyzers, together with LiCor's analysis interface unit, were used to collect and store observations of changing [H_2O], [CO_2] and [CH_4], air temperature, air pressure, PAR (LiCor Inc., LI-190) and both hummock and hollow *Sphagnum*/peat temperatures (~5 cm below their respective surface) in one-second intervals for 400 s (Fig. 2). The 400 s duration allows for clear CO_2 and CH_4 concentration trends. Longer sampling intervals were not desirable in this system because they: (1) were unnecessary to obtain linear changes in gas concentration and repeatable flux values, (2) lead to increased internal concentrations which could exacerbate leaks if present, (3) result in large changes in chamber water vapor concentration which may impair the function of the CH_4 analyzer, and (4) result in large changes in air temperature under daylight conditions (further discussed below). A fitted opaque plastic cover (Fig. 1) was manufactured to cover the transparent enclosure and allow measurements of community respiration.

Measurements

Flux measurements and calculations

Individual flux measurements began when the transparent enclosure was clamped to the permanent collar and data logging was initiated in the LI-7500A (LiCor Inc., Lincoln, NE) interface unit. A typical measurement series (Fig. 2) included observations in full

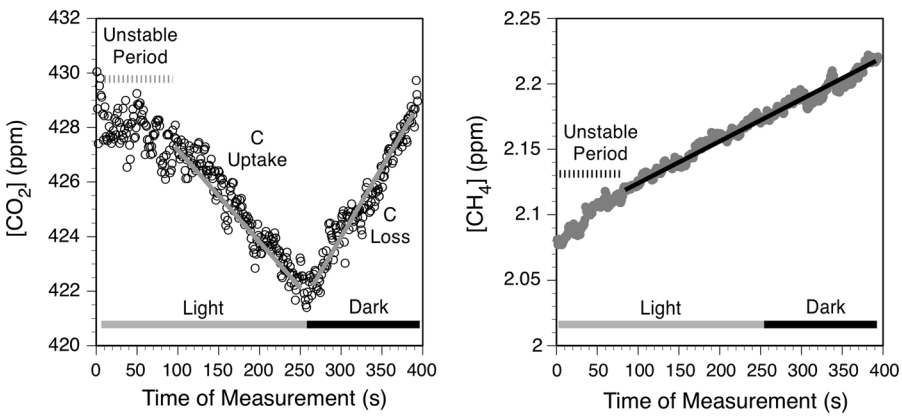

Fig. 2 A typical time sequence of CO_2 and CH_4 concentrations within the enclosure during a measurement including the transition from daylight to dark conditions around 250 s. *Straight lines* over the measured data represent the linear regression slopes calculated to estimate gas flux

ambient light (~200 s) and darkened conditions (~200 s).

Following field data collection, the rate of change in the concentration of each gas within the chamber headspace was calculated using the following equation:

$$CX_x\ Flux = d[CX_x]/dt \times Vol/Area \quad (1)$$

where CX_x *Flux* is in μmol m^{-2} s^{-1}, $[CX_x]$ is in μmol mol^{-1}, *t* is in seconds, $d[CX_x]/dt$ is the slope of the change in concentration, *Vol* is the volume of the enclosure above the bog surface (converted and calculated in moles of dry air), as calculated with base area and the distance from chamber top to peat surface, and *Area* is the planar area (a constant 1.13 m^2) of the bog surface encircled by the permanent collar. The height of the chamber is 1.6 m. Individual measurement periods were rejected if linear relationship for CO_2 or CH_4 had an $r^2 < 0.9$, as suggested for traditional non-steady state non-flow through chamber approach (Song et al. 2009). All values of measured $[CX_x]$ were corrected for the dilution effect caused by increasing water vapor concentrations within the enclosure during the measurement interval (LiCor 2010). To keep reported gas flux at the land–atmosphere interface consistent in this study, we used positive flux to represent gas loss to the atmosphere and negative values for gas uptake by the terrestrial ecosystem.

A typical measurement sequence for $[CX_x]$ produced concentration changes of no more than ±10 μmol mol^{-1} for CO_2, and no more than +2 μmol mol^{-1} for CH_4 from the initially enclosed ambient air concentrations. These levels of change are much lower than gradients produced in small diameter collars with low equilibration volumes. Enclosure air temperature changes under zero- or low-light conditions were negligible, and limited to changes within +2 °C of ambient for direct sunlight exposures. Periodic leak tests of the transparent enclosure clamped to a blank reference plate were conducted by elevating the internal $[CO_2]$ of the enclosure (~800 μmol mol^{-1}). Such tests showed no change in $[CO_2]$ over several minutes for these extreme differential conditions. Internal and external pressures were measured independently inside (LiCor LI-7700 pressure sensor) and outside (LI-7550 pressure sensor) of the chamber and found to be stable during the measurement periods defined in Fig. 2.

Throughout 2011, 2012 and early portions of 2013, flux observations were collected at periodic intervals on two replicate collars near but outside the SPRUCE treatment plots in the S1-Bog. In 2013, 16 new collars were added to each SPRUCE experimental plot established on the S1-Bog. Following the installation of the 16 we discontinued use of the original two. We used the 16 collars to evaluate spatial heterogeneity in peat CO_2 and CH_4 fluxes across the SPRUCE treatment plots. This paper includes all measurements conducted before the onset of sustained SPRUCE heating treatments in 2014. Measurements were collected in August, September and October 2011; monthly from May through November 2012; July, September and October 2013; and June and July 2014. Plots continued to be assessed from September–December 2014 to include the early winter period with frozen *Sphagnum* surfaces (December 2014). The combined data set covers a wide range of peat temperatures (−6 to 24 °C at the *Sphagnum* surface) and seasonally dynamic patterns. S1-Bog CO_2 and CH_4 flux data from 2011 through 2014 are archived in a long-term repository (Hanson et al. 2014a).

Bog environmental measurements

Multipoint thermistor probes were custom designed to measure temperature throughout the peat profile (W.H. Cooke and Co. Inc, Hanover, PA). Peat temperatures were recorded every 30 min at 7 depths near the two initial test collars located outside SPRUCE treatment plots (0, −5, −20, −40, −80, −160 and −200 cm beneath the hollow surface) and at 9 depths within the designated SPRUCE experimental plots (0, −5, −10, −20, −30, −40, −50, −100 and −200 cm). Hummock temperature measurements were also obtained at various elevations above the hollow surface (0 and +10–15 and +20–25 cm). These continuous measurements supplement the hummock and hollow peat temperature measurements (each approx. −5 cm below their respective surface) made within each collar throughout each flux measurement period. The custom integrated probes were manufactured from a 1.3 cm diameter × 0.9 mm wall stainless steel tube. A 7.62 cm stainless steel disk was welded at the zero height position along the tube, and an electrical termination enclosure was supported above the bog surface by a 46 cm extension of the measurement tube to keep it above any standing water

and to avoid shading the bog surface at the point of measurements.

Air temperature and relative humidity measurements were made with a combination sensor (Viasala, Finland; Model HMP155A) and monitored at 0.5, 1, and 2 m above the bog surface in the center of each plot location.

Water table height measurements were automatically recorded every 30 min with water level probes having 1 mm resolution (Trutrack Ltd. Christchurch, New Zealand; Part No. WT-VO2000) installed in a 5.25 cm diameter well casing. Wells were located within 2 m of the flux collar.

Photosynthetically active radiation (PAR) was measured with quantum sensors (LiCor Inc., LI-190) in three distinct locations beside those in the chambers: (a) 2 m above the surface away from shading trees, (b) at shrub heights ($\sim$+30 cm)], and (c) near the *Sphagnum* surface with underwater PAR sensors (LiCor Inc., LI-192) to allow data collections and instrument performance during flooded conditions.

All data collections were controlled and recorded on an automated data logger (Campbell Scientific, Inc. Logan, UT; CR1000). S1-Bog environmental measurement data from 2010 through 2014 are archived in a long-term repository (Hanson et al. 2014b).

Ground-level C flux assessments

Annual carbon cycle flux

Seasonal flux data for both gases and all years of observation were combined and fitted to regression equations for use in the interpolation of annual NEE for the S1-Bog. The community respiration was fit to the following temperature response equation:

$$CO_2ER = BASE_{CO_2} \times Q_{10CO_2}{}^{\wedge}((T_x - T_{ref})/10) \quad (2)$$

where CO_2ER is the exchange rate of CO_2 in μmol m^{-2} s^{-1}, $BASE_{CO_2}$ the exchange rate at the reference temperature, Q_{10CO_2} is the apparent temperature response for a 10 K change in temperature, T_x is the peat temperature in K at a known depth (x), and T_{ref} is the temperature associated with measured base CO_2ER value (288.15 K).

The CH_4 flux was fit to an expanded temperature response equation that includes a modifier for the influence of changing water table depth (Dise et al. 1993):

$$CH_4ER = BASE_{CH_4} \times Q_{10CH_4}{}^{\wedge}((T_x - T_{ref})/10) \times (WT_{frac}) \quad (3)$$

$$WT_{frac} = WT \times a + b$$

where CH_4ER is the exchange rate of CH_4 in μmol m^{-2} s^{-1}, $BASE_{CH_4}$, Q_{10CH_4}, T_x and T_{ref} are analogous to the CO_2 flux parameters defined previously. WT_{frac} is a 0–1 multiplier that captures the influence of declining water table depths on CH_4 efflux from the bog. WT is the water table depth below the hollow height in mm, and a and b are constants (obtained from nonlinear regression). More mechanistic expressions for CH_4 efflux are available that characterize both production and oxidation and a variety of transport pathways (Walter and Heimann 2000; Zhuang et al. 2004; Tian et al. 2010; Wania et al. 2010; Riley et al. 2011), but here we use a simple empirical relationship to estimate annual flux rates from the data set. Such mechanistic expressions will be employed for the future interpretation of CH_4 flux from the planned SPRUCE experiment when additional ancillary driver data sets become available (e.g., substrate availability from current dissolved organic carbon (DOC) production, oxidation processes in aerated peat and additional observations of water table depth and thus aeration of the peat profile).

Of all peat temperature depths assessed, peat temperatures 10 cm below the bog surface explained the most variation in CO_2 and CH_4 flux rates described in Eqs. 2 and 3. Combining half-hour temperature data with the fitted flux relationships projected annual patterns of flux were estimated for the S1-Bog in 2011, 2012, 2013 and 2014.

Daylight measurements (uncovered) were used to estimate whole-ecosystem net exchange of CO_2 during ambient daylight conditions. The following empirical equation for a light response curve (Hanson et al. 1987) was fitted to such data to quantify light saturated rates of CO_2 uptake by the bog vegetation complex and the light levels required for photosynthesis to exceed whole-system C losses.

$$CER = P_{sat} \times \left[1 - (1 - R_{com}/P_{sat})^{\wedge}(1 - PAR/LCP)\right] \quad (4)$$

where CER in μmol CO_2 m^{-2} s^{-1} is the net CO_2 exchange rate over the bog community. CER differs from the commonly characterized NEE because tree stem and foliage CO_2 exchange present in this

Table 1 Regression coefficients (±95 % CI) for fitted relationships between CO_2 and CH_4 flux rates and their respective environmental drivers as inferred from Eqs. 2, 3 and 4

Regression equation	Regression coefficients							
	$Base_{CX_x}$ at T_{ref} (μmol CX_x m^{-2} s^{-1})[a]	Q_{CH_X} (unitless)	a (unitless)	*b* (unitless)	*Psat* (μmol CO_2 m^{-2} s^{-1})	R_{eco} (μmol CO_2 m^{-2} s^{-1})	LCP (μmol quanta m^{-2} s^{-1})	R^2
Dark CO_2 flux × temperature at 0 cm [Eq. 2]	4.2 ± 0.3	2.1 ± 0.3	NA	NA	NA	NA	NA	0.57
CH_4 flux × temperature at −20 cm and water table depth [Eq. 3]	0.179	6.3 ± 2.3	−0.002	0.624	NA	NA	NA	0.45
	Not constrained		Not constrained	Not constrained				
Net daylight CO_2 flux × PAR [Eq. 4] when peat surface temperatures are below 10 °C	NA	NA	NA	NA	−4.6 ± 1.9	1.7 ± 0.4	180 ± 54	0.50
Net daylight CO_2 flux × PAR [Eq. 4] when peat surface temperatures are above 10 °C	NA	NA	NA	NA	−6.1 ± 0.8	5.0 ± 0.4	167 ± 23	0.68

NA not applicable

[a] T_{ref} for these equations was 288.15 K

ecosystem are excluded. P_{sat} in μmol CO_2 m^{-2} s^{-1} is the light saturated rate of net CO_2 uptake, R_{com} in μmol CO_2 m^{-2} s^{-1} is the community CO_2 loss rate to the atmosphere under dark conditions (i.e., apparent community respiration), and *LCP* in μmol quanta m^{-2} s^{-1} is the light compensation point where R_{eco} is balanced by net ecosystem photosynthesis. Parameter values and R^2 information for the fitted empirical regression equations for Eqs. 2, 3 and 4 are provided in Table 1.

Statistical analyses

Means for CO_2 and CH_4 flux were calculated and nonlinear regression statistics (IBM SPSS Statistics Version 21) were used to fit the available data to Eqs. 2, 3 and 4. Box-and-whisker plots characterizing spatial variation within a sampling date were generated with DeltaGraph Version 6.0.18.

Results

Measured CO_2 and CH_4 flux

Community level flux of CO_2 and CH_4 under dark conditions showed the anticipated annual cycle with maximum efflux in July and August when peat temperatures reached their annual peak, and near zero efflux to the atmosphere during frozen winter periods (Fig. 3). CO_2 efflux from the community ranged from a mean of 0.4 μmol m^{-2} s^{-1} when soils were frozen, to peak midsummer values between 6–8 μmol m^{-2} s^{-1}. Higher efflux rates were occasionally observed for individual collars, but they exceeded the mean fitted response to Eq. 2 and were not representative of the majority of S1-Bog CO_2 efflux rates. These seasonal patterns were consistent over the 4 years of observations.

Net CO_2 exchange rates were dependent on ambient light conditions (Fig. 4). The autotrophic shrub, forb, sedge and *Sphagnum* moss community took up CO_2 when PAR reached 194 μmol quanta m^{-2} s^{-1} and became light saturated above 1000–1200 μmol quanta m^{-2} s^{-1}. The light-saturated maximum declined by approximately 60 % at temperatures below 10 °C (Fig. 4, grey symbols). Light saturated net photosynthesis reached maximums approaching −6 and −4 μmol CO_2 m^{-2} s^{-1} in the warm and cool

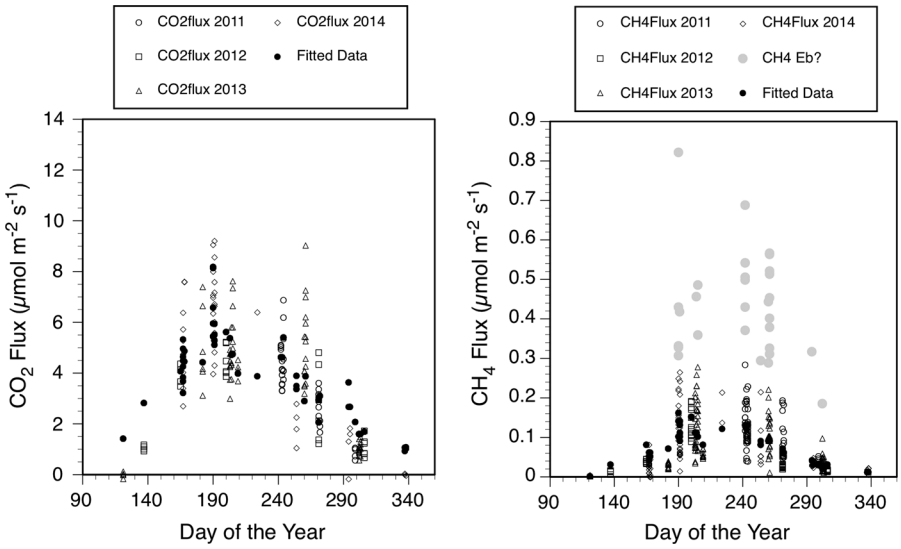

Fig. 3 Periodic observations of dark-daytime CO_2 (*left graph*) and CH_4 (*right graph*) efflux measured throughout the active seasonal cycle for the S1-Bog. *Data* represent the combined observations from measurements collected from variable plot locations on the S1-Bog in 2011, 2012, 2013 and 2014. Fitted values from Eqs. 2 and 3 are also *plotted* in each graph. A subset of the CH_4 flux data that exceeded one standard deviation of the mean for a given temperature range (CH4 Eb?—possible ebullition) are highlighted from the rest of the data

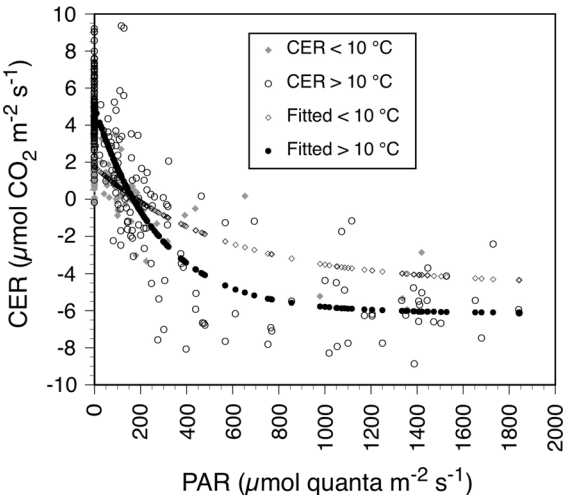

Fig. 4 Net community CO_2 exchange for the collared area under ambient light conditions. Negative values represent CO_2 uptake from the atmosphere to the bog. *Gray solid diamonds* and *open circles* represent data collected at surface peat temperatures below or above 10 °C. The *open diamonds* and *black circles* are the fitted data for the data obtained below and above the 10 °C surface soil temperatures

periods of the growing season (Fig. 4). These levels of community NEE were a bit higher than the bog data reported by Frolking et al. (1998), but in the middle of the range for rich fens. The data for Frolking et al. (1998) include peatlands at a higher latitude with cooler temperature regimes, which may explain in part why the S1-Bog rates are higher (i.e., higher overall activity combined with potentially greater nutrient availability).

Instantaneous CH_4 efflux rates did not vary during imposed light to dark transitions (Fig. 2) and we report flux data throughout the entire 400 s measurement period. The mean CH_4 efflux ranged from 0.01 μmol m^{-2} s^{-1} when the bog surfaces were frozen or covered with snow to maximum rates between 0.15 and 0.25 μmol m^{-2} s^{-1} (Fig. 3). Peak rates in summer months ranged between 0.3 and 0.5 μmol m^{-2} s^{-1}, roughly an order of magnitude less than mid-summer CO_2 exchange rates. As for CO_2, higher CH_4 efflux rates were occasionally observed for individual collars, but they exceeded the mean fitted response to Eq. 2 and were not representative of the majority of S1-Bog CH_4 efflux rates.

Spatial variation in 'dark' CO_2 and CH_4 efflux Across the S1-Bog

During near-freezing cold periods (0–2 °C at −10 cm; October 2013), we saw limited spatial variation in CO_2 and CH_4 flux across all 16 SPRUCE plot collars in the

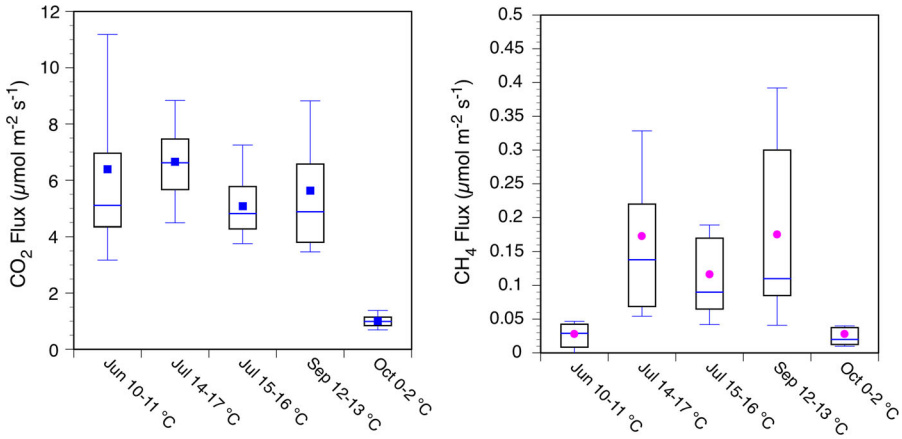

Fig. 5 Spatial variation statistics in "dark condition" CO_2 flux (*left graph*) and CH_4 flux (*right graph*) for multiple locations across a 2.6 ha experimental area at the south end of the S1-Bog. The box-and-whisker plots capture 10, 25, 75 and 90th percentiles of the spatial data along with the overall median (50th percentile) and the symbol is the mean of the spatial data set. Individual plots were deployed 20–30 m apart along three transects within this area. Data are plotted for June 2014, July 2014, July 2013, September 2013 and October 2013 sampling periods which cover a full seasonal range of peat temperatures (−10 cm reference temperature depth)

S1-Bog (Fig. 5). Under warmer conditions, CO_2 efflux under dark conditions showed considerable variation that was strongly associated with temperature. In July 2013 and 2014, with peat temperatures ranging between 14 and 17 °C, CO_2 efflux rates were typically 4–7 μmol CO_2 m^{-2} s^{-1} with divergent collars showing flux above 8 μmol CO_2 m^{-2} s^{-1}. In September 2013, with peat temperatures between 12–13 °C, collar flux were between 3 and 7 μmol CO_2 m^{-2} s^{-1} and divergent high flux values still exceeded 6–8 μmol CO_2 m^{-2} s^{-1}. A single collar exhibited a flux rate of greater than 13 μmol CO_2 m^{-2} s^{-1}.

CH_4 flux for warmer conditions (June 2014 and July 2013 and 2014) showed typical rates between 0.05 and 0.1 μmol CH_4 m^{-2} s^{-1} with divergent flux up to 0.5 μmol CH_4 m^{-2} s^{-1}. During June 2014 (surface temperatures from 10 to 11 °C) at a time when bog photosynthetic activity was just recovering from a long winter, the spatial variation of CH_4 flux across the bog was still muted (Fig. 5). Mid-season maximum flux rates and increased spatial variation may be driven in part by spatial variation in current photosynthate supplies reaching belowground microbial systems through root turnover or exudation processes.

There was not a direct correlation among collar locations exhibiting high CO_2 and CH_4 flux, which suggests that in situ bog processes were driving these efflux rates. If a biased technical approach had been responsible for the divergent flux rates one might expect both the CO_2 and the CH_4 flux rates to parallel one another.

Interpolation of point-in-time data to annual CO_2 or CH_4 efflux

CO_2 and CH_4 flux by temperature relationships were used to approximate annual C fluxes (Fig. 6; Eqs. 2, 3). Although these simple empirical relationships averaged across multiyear data sets captured only a portion of the observed variation in the data (see Table 1 R^2 values), they can be used to generate integrated annual net exchange for the bog for each gas. For environmental conditions from 2011 to 2014, mean net CO_2 efflux for dark conditions was estimated to range from 865 to 937 g CO_2–C m^{-2} y^{-1} and estimated CH_4 flux ranged from 15 to 18 g CH_4–C m^{-2} y^{-1}. The calculated annual C flux for each showed CO_2-C flux to be 52–62 times greater than CH_4-C efflux from the bog ecosystem. This is in the same range as the ratio of flux estimated from the instantaneous data (see Figs. 3, 6). It should be acknowledged that fitted values from Eq. 2 overestimate mean CO_2 efflux when peat temperatures fall below 1 °C, and therefore the annual interpolations of bog CO_2 efflux from Eq. 2 may be a bit high during mid-winter periods.

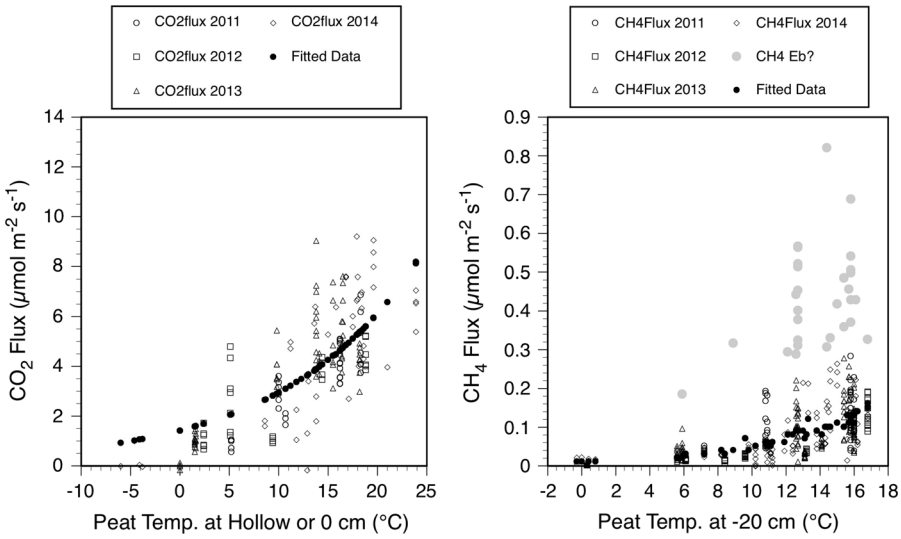

Fig. 6 The relationship between CO_2 community respiration (*left graph*) and CH_4 efflux (*right graph*) to peat temperatures at 0 cm for CO_2 and −20 cm for CH_4 for the combined data set collected in 2011, 2012, 2013 and 2014. The *small black points* in each plot represent the fitted apparent temperature response functions described in the text. CH_4 efflux values exceeding one standard deviation of a temperature range within the combined data set (CH_4 Eb?—possible ebullition) were not used to establish the fitted relationship and are further discussed in the text

We estimated that annual gross CO_2 uptake by shrubs, forbs, and *Sphagnum* to range from −857 to −956 gCO_2–C m^{-2} y^{-1} (interpolated from Fig. 4 data). Such rates of carbon uptake by the vegetation community were masked by the collar community respiration losses also ranging from 865 to 937 gCO_2–C m^{-2} y^{-1}. Respiration from the collars may include contributions from tree roots within the plot, although the collars themselves did not include any trees. Total NEE of carbon showed a very small uptake of −3.1 gCO_2–C m^{-2} y^{-1} estimated for 2013, but C losses to the atmosphere ranging from 21 to 65 gCO_2–C m^{-2} y^{-1} for the other years. Tree contributions to gross photosynthetic uptake, which were not evaluated in this paper, may be responsible for tipping the carbon balance for the bog to a carbon sink (Jensen et al. 2015).

Discussion

Application of the large-collar method to a peatland and comparisons to other studies

The community-level approach to the quantification of CO_2 and CH_4 exchange was capable of capturing both seasonal (Fig. 3) and temperature-driven (Fig. 6) patterns of dark efflux and the net daytime exchange of CO_2 as it varies with ambient light conditions (Fig. 4). The absolute range of the observed flux from near zero to maximum midseason values correlated with high midseason peat temperatures (Figure S2), and is consistent with prior published work for similar peatlands (Table 2).

Methane flux from northern bogs in Minnesota (Crill et al. 1988; Dise et al. 1993) and Michigan (Shannon and White 1994) are higher than other more northerly and cooler Canadian bog ecosystems (Lai et al. 2014a, b; Roulet et al. 2007; Blodau et al. 2007; Moore and Knowles 1990). The large collar method is capable of characterizing spatially variable CH_4 flux rates within the S1-Bog in Minnesota (Fig. 5). The spatial variability in flux rates suggests strong heterogeneity of belowground microbial activity, which will be an important process to consider as we evaluate ecosystem responses to the experimental treatments.

The measured data on simultaneous CO_2 and CH_4 flux confirm the predominance of CO_2 over CH_4 efflux as a form of heterotrophic C emissions from the S1-Bog. Such observations have been observed previously on the Marcell Experimental Forest (Olson et al. 2013), in a Michigan Fen (Ballantyne et al. 2014), Ontario bogs (Blodau et al. 2007; Roulet et al. 2007) and similar bogs outside of North America (see

Table 2 CO_2 and CH_4 flux observations from wetlands in comparable temperate climate zones

Location Latitude	Ecosystem type	Method	Peat depth (m)	Temperature mean annual (°C)	Temperature maximum (°C)	Maximum community respiration (μmol m^{-2} s^{-1})	Maximum CH_4 flux (μmol m^{-2} s^{-1})	References
Minnesota 47°30′N	**Bog**	**Community chamber**	**3**	**4.5**	**18**	**6–10**	**0.3–0.5 (peaks)** **0.15–0.2**	**This study**
Minnesota 47°32′N	Bog	Chambers	>3	3	15–16	–	0.43–0.48	Crill et al. (1988)
Minnesota 47°32′N	Bog Fen	Chambers	>3	3	10–11	–	0.03–0.18 0.35	Dise (1993)
Minnesota 47°32′N	Bog Fen	Chambers	3	3.1	20–21	–	0.69 0.55	Dise et al. (1993)
Minnesota 47°30′N	Fen	Eddy Flux	3	3	18.5	4–5	0.22–0.29 (peaks) 0.078-0.123	Olson et al. (2013)
Minnesota 47°32′N	Fen	Eddy flux	3	3	15–16	–	0.27 (Eb.) 0.1	Shurpali et al. (1993)
Minnesota 47°32′N	Fen	Eddy flux	3	3	15–16	–	0.1–0.13	Shurpali and Verma (1998)
Michigan 42°27′N	Bog Fen	Chambers	NA	~10	20–25	–	0.91	Shannon and White (1994)
Michigan 46°19′N	Fen	Chambers	1.1–1.3	5.1	NA	2.1–3.0 (mean)	0.002–0.011	Ballantyne et al. (2014)
Ontario 45°25′N	Bog	Chambers	5–6	6	NA	–	0.7 (peak) 0.02	Moore et al. (2011)
Ontario 45°41′N	Bog	Chambers	5–6	6	NA	–	0.6 (peak)	Lai et al. (2014a, b)
Ontario 45°41′N	Bog	Eddy flux and chambers	4–6	6	20–21	0.5–1	0.06–0.08	Roulet et al. (2007)
Ontario 45°41′N	Bog	Chambers	NA	6	14–15	4.2	0.01–0.03	Blodau et al. (2007)
Quebec 45°33′N	Domed bog	Chambers	1–2	6	20	–	0.17	Moore and Knowles (1990)
Slovenia 45°59′N	Bog undrained	Chambers	NA	10	16	0.9 (mean) 2.8 (max)	0.0005 (mean) 0.003 (max)	Danevcic et al. (2010)

Table 2 continued

Location Latitude	Ecosystem type	Method	Peat depth (m)	Temperature mean annual (°C)	Temperature maximum (°C)	Maximum community respiration (μmol m^{-2} s^{-1})	Maximum CH_4 flux (μmol m^{-2} s^{-1})	References
England 54°65′N	Blanket peat	Chambers	4	10	16	3.2–6.3	0.02–0.06	Mcnamara et al. (2008)
Scotland 55°48′N	Peatland	Chambers	0.5–5	NA	NA	67 ± 18	0.10 ± 0.02	Dinsmore et al. (2009, 2010)
Scotland ~55°05′N	Bog	Chambers	5	~8	~8–10	0.05 (mean) 0.277 (max)	0.01 (mean) 0.05 (max)	Clymo and Pearce (1995)
Ireland 51°55′N	Bog	Chambers	2–3	10.3	NA	–	0.2 (peak) 0.02	Laine et al. (2007)
Ireland 51°55′N	Bog	Chambers	0.5–5	10.6	NA	–	0.01 (mean)	Koehler et al. (2011)
England 54°65′N	Blanket peat	Chambers	4	10	16	3.2–6.3	0.02–0.06	Mcnamara et al. (2008)
Sweden 64°11′N	Mire	Chambers	3–4	1.2	NA	–	0.02–0.04 (mean)	Nilsson et al. (2008)
China 47°35′N	Marsh	Chambers	NA	NA	16.1	–	26 (pulse) 1.7	Song et al. (2012)
China 47°35′N	Marsh	Chambers	>1	2.5	22	9	0.69	Song et al. (2009)

Values in the table shown as approximate were not provided in the original publication, but were derived from other sources

NA not available

additional references in Table 2). Notwithstanding the dominance of CO_2 efflux from the S1-Bog, the greater greenhouse warming potential of CH_4 in the atmosphere justifies its inclusion in peatland measurement protocols (Myhre et al. 2013). Nisbet et al. (2014) have recently highlighted substantial natural and anthropogenic uncertainties in the global methane budget and called for more data to resolve patterns of atmospheric methane concentration increases through time. Indeed, the balance between CO_2 and CH_4 exchange for a wetland determines its greenhouse gas budget (Whiting and Chanton 2001). While northern peatlands have maintained a net cooling influence throughout the Holocene (Frolking and Roulet 2007), changes in the balance of CO_2 and CH_4 emissions associated with SPRUCE experimental treatments will lead to important information about the future role of peatlands in the global climate system.

Dise et al. (1993) provided independent models for CH_4 efflux from hollow and hummock bog locations for a nearby MEF bog that overlap the fitted data (Eq. 3) from the community-level measurement approach reported in this paper (Figure S1). Such agreement confirms that this new approach reproduces expected ground area flux estimates for regional peatlands, and suggests that it is a viable method for comparing and contrasting both CO_2 and CH_4 flux from manipulated warming treatment plots.

Characteristics of the measurement method

With ideal conditions, the transparent enclosure and analyzer column can be transported among and used on eight collars in a 4–6 h measurement day (midday period) in our current protocol that allows for repeated observations on each collar. High humidity following rain events coupled with cold instrument surfaces during early morning observations have combined to cause individual measurement failures due to the formation of condensation on the surface of the CH_4 and CO_2 sensor mirrors. Because of the open path nature of CO_2 and CH_4 sensors, stray leaves or insects may also interfere with the measurement pathway and invalidate results, but this is not a common issue. Pressure differences within and out of the enclosed space were recorded and found to be inconsequential.

Lai et al. (2012) recently reported on the influence of atmospheric turbulence and measurement periods pertinent to the use of auto-chambers for surface flux measurements from peatlands. They concluded that surface boundary layer disturbance can produce flux divergences and should be minimized. This phenomenon is well known for closed chamber observations of CO_2 efflux from mineral soils (Hanson et al. 1993; Christiansen et al. 2011; Koskinen et al. 2014), and is the reason air is mixed in the upper portion of the chamber only. Stirring of the large volume is helpful in providing a stable concentration change with time, but too much stirring too close to the bog surface would disturb the boundary layer and over predict short term flux. Pihlatie et al. (2013) recently conducted a comparison of a range of static chamber measurements for CH_4 emissions from soils and controlled conditions. They concluded that larger chamber volumes avoided some of the biases of smaller chamber volumes. Our system with a large volume provides these advantages.

Levy et al. (2011) contrasted various methods for interpreting the rate of change of gases within static chambers and found different results using a variety of methods including linear and nonlinear approaches. The change in chamber CO_2 and CH_4 concentrations is small and linear during our short term flux measurements, and a linear regression approach was used to characterize the rate of gas emission. Moreover, Venterea and Parkin (2012) recommended a few ultimate solutions to eliminate the bias: (1) very short deployment period of chamber, (2) large chamber height, (3) advances in measurement instrumentation with high precision and high sensitivity, and (4) real-time in situ analysis. These suggested solutions, along with the large chamber base area to cover the hummock and hollow microtopography, are widely accepted advantages of our method.

On balance, the characteristics of the current method as compared with common static chamber methods that might be considered advantageous include: (1) its application to the full community complexity of an in situ system, (2) short term (6–7 min), real-time dual gas concentration measurements which reduce biases caused by gas leakage and changes of in-chamber temperature and moisture during measurement, and (3) the use of accurate and durable analyzers in the field. With appropriate consideration of the need for a large-footprint flux observation, this approach could easily be applied in other vegetation types.

A couple of possible disadvantages of the approach should also be mentioned: (1) the short measurement period could cause biases because the gas inside the chambers may not be in equilibrium, and (2) temporal variation in emissions may not be captured by the point-in-time approach. Performance of the large-collar chamber will be compared to other automatic static chambers as well as ambient eddy covariance approaches in the future.

Annual C efflux

Extrapolation of our chamber data for meteorological conditions for the years between 2011–2014 showed mean ± SD annual "dark" CO_2 and CH_4 efflux from the S1-Bog to be 894 ± 34 and 16 ± 2 gC m^{-2} y^{-1}, respectively. The methane loss rates are comparable in magnitude to dissolved organic carbon losses estimated for the S1-watershed (Steve Sebestyen, personal communication). Roulet et al. (2007) estimated cumulative annual CH_4-C losses from the Mer Bleue bog in Ontario of only 3.7 gC m^{-2} y^{-1}, although Mer Bleue is a drier bog with a growing season water table 30–40 cm below the surface. Bubier et al. (1993) reported a wider range from 0.06 to 10.1 gC m^{-2} y^{-1} for a range of northern Ontario peatlands. In an extensive synthesis of data for a broad range of European peatlands Carter et al. (2012) also recorded annual CH_4 flux to be between 0.5 to 6.8 gCH_4–C m^{-2} y^{-1}.

Estimated night CO_2-C losses from the S1-Bog are over 40 times higher than the CH_4-C losses, suggesting a minimal role for CH_4-C efflux in the overall NEE from the bog. However, unlike the absolute loss of CH_4-C, substantial CO_2 is also taken into the bog via photosynthesis during warm (i.e., above freezing) daylight growing season periods (see "Interpolation of point-in-time data to annual CO_2 or CH_4 efflux" section). When the night CO_2 losses are offset by annual uptake of CO_2–C by bog vegetation, the disparity between CO_2–C and CH_4–C losses is reduced to only a fivefold to sixfold difference. If we were to factor in the contribution of the S1-Bog's tree photosynthesis (not addressed in this paper), annual CH_4 emissions might dominate net C losses from the peatland.

The S1-Bog and other peatlands on the MEF yield CH_4 at a higher rate than many other studied bogs. Warmer peat temperatures, a deep peat column with shallow water table, and substantial supplies of dissolved organic carbon substrates for methanogens from the established tree, shrub and peat communities on the MEF bogs may all help explain this enhanced rate of efflux observed here and in prior work (Crill et al. 1988; Dise 1993; Dise et al. 1993; Tfaily et al. 2014). Song et al. (2009) reported annual interpolations of CO_2 and CH_4 flux for a permanently inundated marsh in China of 513 and 39 gC m^{-2} y^{-1}, respectively, which is comparable to the rates observed for the S1-Bog. Methane flux at the S1-Bog is at the high end of the range of flux reported for organic soil sites in the United Kingdom (Levy et al. 2012).

A limitation of current empirical models for estimating seasonal flux is that they do not allow for variations in the contributions of differing substrates to the microbial communities responsible for much of the CO_2 and CH_4 flux. The empirical models applied in this study are missing logical mechanistic contributions that might be driven by measured substrate supply and variable microbial community response. Such details will be resolved in future applications of the method.

Conclusions

Based on 4 years of observational flux measurements, the S1-Bog site for the SPRUCE project is found to be representative of temperate peatlands in terms of CO_2 and CH_4 flux. As such, these observations, provide a practice foundation for the planned experimental manipulations including whole ecosystem warming and elevated CO_2 treatment. The measured CO_2 and CH_4 flux in S1-bog is specifically appropriate to the interpretation of C flux dynamics from non-permafrost peatlands at the southern end of the boreal forest region.

Integrating the observational data from the SPRUCE project with process-based models will be valuable for mechanistic understanding of the biogeochemical processes in peatlands and their responses to the climate warming and elevated atmospheric CO_2 and thereby allow for future predictive understanding of important greenhouse gas flux from peatlands. Our method for community-level CO_2 and CH_4 flux observations from large-diameter collars produced repeatable flux data in agreement with traditional methods. The data were in agreement to prior flux data

for warm-location raised-bog peatlands in southern portions of the boreal forest. The method is field portable and deployable to multiple locations, and is a viable method for long-term repeated evaluations of CO_2 and CH_4 flux under naturally variable conditions. Pairing this method with more traditional small-collar data collections for selected hummock or hollow zones, with high temporal resolution data capable of capturing ebullitive processes (Bridgham et al. 2013), or nesting in within a larger eddy covariance foot print would enable further mechanistic details to be resolved.

Acknowledgments The S1-Bog CO_2 and CH_4 flux data (Hanson et al. 2014a) and the environmental measurement data referenced in this paper are archived at, and available from, the SPRUCE long-term repository (http://www.mnspruce.ornl.gov).This material is based upon work supported by the U.S. Department of Energy, Office of Science, Office of Biological and Environmental Research, and Graduate Fellowship Program (DE-AC05-06OR23100 to A. L. G.). Oak Ridge National Laboratory is managed by UT-Battelle, LLC, for the U.S. Department of Energy under contract DE-AC05-00OR22725.The authors appreciate fieldwork participation of W. Robert Nettles and Cassandra Ott, and would like to thank Scott Bridgham, Jeff Chanton, Steve Sebestyen, Nigel Roulet and Tim Moore for their comments on earlier versions of this manuscript. We also thank Terry Pfeiffer for her editorial assistance.

Open Access This article is distributed under the terms of the Creative Commons Attribution 4.0 International License (http://creativecommons.org/licenses/by/4.0/), which permits unrestricted use, distribution, and reproduction in any medium, provided you give appropriate credit to the original author(s) and the source, provide a link to the Creative Commons license, and indicate if changes were made.

References

Arnone JA III, Obrist D (2003) A large daylight geodesic dome for quantification of whole-ecosystem CO_2 and water vapor fluxes in arid shrublands. J Arid Environ 55:629–643. doi:10.1016/S0140-1963(02)00291-4

Baird AJ, Belyea LR, Morris PJ (2009) Upscaling peatland-atmosphere fluxes of carbon gases: small-scale heterogeneity in process rates and the pitfalls of 'bucket-and-slab' models. In: Baird AJ, Belyea LR, Comas X, Reeve A, Slater L (eds) Northern peatlands and carbon cycling, vol 184. American Geophysical Union, Washington DC, pp 37–54

Ballantyne DM, Hribljan JA, Pypker TG, Chimner RA (2014) Long-term water table manipulations alter peatland gaseous carbon fluxes in Northern Michigan. Wetlands Ecol Manag 22:35–47

Barbier C, Hanson PJ, Todd DE Jr, Belcher D, Jekabson EW, Thomas WK, Riggs JS (2012) Air flow and heat transfer in a temperature controlled open top enclosure. ASME International Mechanical Engineering Congress and Exposition, Houston **(Paper #IMECE2012-86352)**

Belyea LR, Baird AJ (2006) Beyond "the limits to peat bog growth": cross-scale feedback in peatland development. Ecol Monogr 76:299–322

Blodau C, Roulet NT, Heitmann T, Stewart H, Beer J, Lafleur P, Moore TR (2007) Belowground carbon turnover in a temperate ombrotrophic bog. Glob Biogeochem Cycles 21:GB1021. doi:10.1029/2005GB002659

Bridgham S, Cadillo-Quiroz H, Keller JK, Zhuang Q (2013) Methane emissions from wetlands: biogeochemical, microbial, and modeling perspectives from local to global scales. Glob Change Biol 19:1325–1346. doi:10.1111/gcb.12131

Bubier JL, Moore TR (1994) An ecological perspective on methane emissions from northern wetlands. Trends Ecol Evol 9:460–464. doi:10.1016/0169-5347(94)90309-3

Bubier JL, Moore TR, Roulet NT (1993) Methane emissions from wetlands in the midboreal region of Northern Ontario, Canada. Ecology 74:2240–2254. doi:10.2307/1939577

Carter MS, Larsen KS, Emmett B, Estiarte M, Field C, Leith ID, Lund M, Meijide A, Mills RTE, Niinemets Ü, Peñuelas J, Portillo-Estrada M, Schmidt IK, Selsted MB, Sheppard LJ, Sowerby A, Tietema A, Beier C (2012) Synthesizing greenhouse gas fluxes across nine European peatlands and shrublands—responses to climatic and environmental changes. Biogeosciences 9:3739–3755. doi:10.5194/bg-9-3739-2012

Christiansen JR, Kornhonen JFJ, Juszczak R, Giebels M, Pihlatie M (2011) Assessing the effects of chamber placement, manual sampling and headspace mixing on CH_4 fluxes in a laboratory experiment. Plant Soil 343:171–185. doi:10.1007/s11104-010-0701-y

Clymo RS, Pearce DME (1995) Methane and carbon dioxide production in, transport through, and efflux from a peatland. Philos T R Soc A 351:249–259. doi:10.1098/rsta.1995.0032

Crill PM, Bartlett KB, Harriss RC, Gorham E, Verry ES, Sebacher DI, Madsar L, Sanner W (1988) Methane flux from Minnesota peatlands. Glob Biogeochem Cycles 2:371–384. doi:10.1029/GB002i004p00371

Danevcic T, Mandic-Mulec I, Stres B, Stopar D, Hacin J (2010) Emissions of CO_2, CH_4, and N_2O from Southern European peatlands. Soil Biol Biochem 42:1437–1446. doi:10.1016/j.soilbio.2010.05.004

Dinsmore KJ, Skiba UM, Billett MF, Rees RM, Drewer J (2009) Spatial and temporal variability in CH_4 and N_2O fluxes from a Scottish ombrotrophic peatland: implications for modelling and up-scaling. Soil Biol Biochem 41:1315–1323

Dinsmore KJ, Billett MF, Skiba UM, Rees RM, Drewer J, Helfter C (2010) Role of the aquatic pathway in the carbon and greenhouse gas budgets of a peatland catchment. Glob Change Biol 16:2750–2762

Dise NB (1993) Methane emission from Minnesota peatlands: spatial and seasonal variability. Glob Biogeochem Cycles 7:123–142. doi:10.1029/92GB02299

Dise NB, Gorham E, Verry ES (1993) Environmental factors controlling methane emissions from peatlands in Northern

Minnesota. J Geophys Res Atmos 98:10583–10594. doi:10.1029/93JD00160

Frolking S, Roulet NT (2007) Holocene radiative forcing impact of northern peatland carbon accumulation and methane emissions. Glob Change Biol 13:1079–1088. doi:10.1111/j.1365-2486.2007.01339.x

Frolking SE, Bubier JL, Moore TR, Ball T, Bellisario LM, Bhardwaj A, Carroll ABP, Crill P, Lafleur PM, McCaughey JH, Roulet NT, Suyker AE, Verma SB, Waddington JM, Whiting GJ (1998) Relationship between ecosystem productivity and photosynthetically active radiation for northern peatlands. Glob Biogeochem Cycles 12:115–126

Gorham E (1991) Northern peatlands: role in the carbon cycle and probable responses to climatic warming. Ecol Appl 1:182–195. doi:10.2307/1941811

Hanson PJ, McRoberts RE, Isebrands JG, Dixon RK (1987) An optimal sampling strategy for determining CO_2 exchange rate as a function of photosynthetic photon flux density. Photosynthetica 21:98–101

Hanson PJ, Wullschleger SD, Bohlman SA, Todd DE (1993) Seasonal and topographic patterns of forest floor CO_2 efflux from an upland oak forest. Tree Physiol 13:1–15. doi:10.1093/treephys/13.1.1

Hanson PJ, Phillips JR, Riggs JS, Nettles WR, Todd DE (2014a) SPRUCE CO_2 and CH_4 flux in the S1-Bog. Carbon Dioxide Information Analysis Center, Oak Ridge National Laboratory, U.S. Department of Energy, Oak Ridge. doi:10.3334/CDIAC/spruce.006

Hanson PJ, Riggs JS, Nettles WR, Dorrance C, Hook LA (2014b) SPRUCE environmental monitoring data: 2010–2014. Carbon Dioxide Information Analysis Center, Oak Ridge National Laboratory, U.S. Department of Energy, Oak Ridge. doi:10.3334/CDIAC/spruce.001

Heijmans MMPD, Mauquoy D, van Geel B, Berendse F (2008) Long-term effects of climate change on vegetation and carbon dynamics in peat bogs. J Veg Sci 19:307. doi:10.3170/2008-8-18368

IPCC (2013) Climate change 2013: the physical science basis. Contribution of Working Group I to the fifth assessment report of the intergovernmental panel on climate change. Cambridge University Press, Cambridge

Jensen AM, Warren JM, Hanson PJ, Childs J, Wullschleger SD (2015) Needle age and season influence photosynthetic temperature response and total annual carbon uptake in mature Picea mariana trees. Ann Bot Lond 166:821–832. doi:10.1093/aob/mcv115

Koehler AK, Sottocornola M, Kiely G (2011) How strong is the current carbon sequestration of an Atlantic blanket bog? Glob Change Biol 17:309–319

Kolka RK, Sebestyen SD, Verry ES, Brooks KN (2011) Peatland biogeochemistry and watershed hydrology at the Marcell Experimental Forest. CRC Press, Boca Raton **488**

Koskinen M, Minkkinen K, Ojanen P, Kämäräinen M, Laurila T, Lohila A (2014) Measurements of CO_2 exchange with an automated chamber system throughout the year: challenges in measuring night-time respiration on porous peat soil. Biogeosciences 11:347–363. doi:10.5194/bg-11-347-2014

Krassovski MB, Riggs JS, Hook LA, Nettles WR, Boden TA, Hanson PJ (2015) A comprehensive data acquisition and management system for an ecosystem-scale peatland warming and elevated CO_2 experiment. Geosci Instrum Methods Data Syst 4:203–213. doi:10.5194/gi-4-203-2015

Lai DYF, Roulet NT, Humphreys ER, Moore TR, Dalva M (2012) The effect of atmospheric turbulence and chamber deployment period on autochamber CO_2 and CH_4 flux measurements in an ombrotrophic peatland. Biogeosciences 9:3305–3322. doi:10.5194/bg-9-3305-2012

Lai DY, Roulet NT, Moore TR (2014a) The spatial and temporal relationships between CO_2 and CH_4 exchange in a temperate ombrotrophic bog. Atmos Environ 89:249–259

Lai DYF, Moore TR, Roulet NT (2014b) Spatial and temporal variations of methane flux measured by autochambers in a temperate ombrotrophic peatland. J Geophys Res Biogeosci 119:864–880. doi:10.1002/2013JG002410

Laine A, Wilson D, KielyG Byrne KA (2007) Methane flux dynamics in an Irish lowland blanket bog. Plant Soil 299:181–193

Levy PE, Gray A, Leeson SR, Gaiawyn J, Kelly MPC, Cooper MDA, Dinsmore KJ, Jones SK, Sheppard LJ (2011) Quantification of uncertainty in trace gas fluxes measured by the static chamber method. Eur J Soil Sci 62:811–821. doi:10.1111/j.1365-2389.2011.01403.x

Levy PE, Burden A, Cooper MDA, Dinsmore KJ, Drewer J, Evans C, Fowler D, Gaiawyn J, Gray A, Jones SK, Jones T, McNamara P, Mills R, Ostle N, Sheppard LJ, Skiba U, Sowerby A, Ward SE, Zielinski P (2012) Methane emissions from soils: synthesis and analysis of a large UK data set. Glob Change Biol 18:1657–1669. doi:10.1111/j.1365-2486.2011.02616.x

LiCor (2010) LI-8100A automated soil CO2 flux system and LI-8150 multiplexer Instruction manual, vol 4. LiCor Inc., Lincoln

McNamara NP, Plant T, Oakley S, Ward S, Wood C, Ostle N (2008) Gully hotspot contribution to landscape methane (CH_4) and carbon dioxide (CO_2) fluxes in a northern peatland. Sci Total Environ 404:354–360. doi:10.1016/j.scitotenv.2008.03.015

Moore TR, Knowles R (1990) Methane emissions from fen, bog and swamp peatlands in Quebec. Biogeochemistry 11:45–61. doi:10.1007/BF00000851

Moore TR, De Young A, Bubier JL, Humphreys ER, Lafleur PM, Roulet NT (2011) A multi-year record of methane flux at the Mer Bleue Bog, Southern Canada. Ecosystems 14:646–657

Myhre G, Shindell D, Bréon FM, Collins W, Fuglestvedt J, Huang J, Koch D, Lamarque JF, Lee D, Mendoza B, Nakajima T, Robock A, Stephens G, Takemura T, Zhang H (2013) Chapter 8: anthropogenic and natural radiative forcing. In: Stocker TF, Qin D, Plattner GK, Tignor M, Allen SK, Boschung J, Nauels A, Xia Y, Bex V, Midgley PM (eds) Climate change 2013 the physical science basis. Contribution of Working Group I to the fifth assessment report of the intergovernmental panel on climate change. Cambridge University Press, Cambridge, pp 659–740. doi:10.1017/CBO9781107415324.018

Nilsson M, Sagerfors J, Buffam I, Laudon H, Eriksson T, Grelle A, Klemedtsson L, Weslien P, Lindroth A (2008) Contemporary carbon accumulation in a boreal oligotrophic minerogenic mire—a significant sink after accounting for all C-fluxes. Glob Change Biol 14:2317–2332

Nisbet EG, Dlugokencky EJ, Bousquet P (2014) Methane on the rise—again. Science 343:493–495. doi:10.1126/science.1247828

Olson DM, Griffis TJ, Noormets A, Kolka R, Chen J (2013) Interannual, seasonal, and retrospective analysis of the methane and carbon dioxide budgets of a temperate peatland. J Geophys Res Biogeosci 118:226–238. doi:10.1002/jgrg.20031

Parsekian AD, Slater L, Ntarlagiannis D, Nolan J, Sebestyen SD, Kolka RK, Hanson PJ (2012) Uncertainty in peat volume and soil carbon estimated using ground-penetrating radar and probing. Soil Sci Soc Am J 76:1911–1918. doi:10.2136/sssaj2012.0040

Pihlatie MK, Christiansen JR, Aaltonena H, Korhonena JFJ, Nordbo A, Rasilo T, Benanti G, Giebels M, Helmy M, Sheehy J, Jones S, Juszczak R, Klefoth R, Lobo-do-Vale R, Rosa AP, Schreiber P, Serça D, Vicca S, Wolf B, Pumpanen J (2013) Comparison of static chambers to measure CH_4 emissions from soils. Agric Forest Meteorol 171:124–136. doi:10.1016/j.agrformet.2012.11.008

Riley WJ, Subin SM, Lawrence DM, Swenson SC, Torn MS, Meng L, Mahowald NM, Hess P (2011) Barriers to predicting changes in global terrestrial methane fluxes: analyses using CLM4Me, a methane biogeochemistry model integrated in CESM. Biogeosciences 8:1925–1953. doi:10.5194/bg-8-1925-2011

Roulet NT, Lafleurs PM, Richard PJH, Moore TR, Humphreys ER, Bubier J (2007) Contemporary carbon balance and late Holocene carbon accumulation in a northern peatland. Glob Change Biol 13:397–411. doi:10.1111/j.1365-2486.2006.01292.x

Sebestyen SD, Dorrance C, Olson DM, Verry ES, Kolka RK, Elling AE, Kyllander R (2011) Chapter 2: long-term monitoring sites and trends at the Marcell Experimental Forest. In: Kolka RK, Sebestyen SD, Verry ES, Brooks KN (eds) Peatland biogeochemistry and watershed hydrology at the Marcell Experimental Forest. CRC Press, New York, pp 15–72

Shannon RD, White JR (1994) A three-year study of controls on methane emissions from two Michigan peatlands. Biogeochemistry 27:35–60. doi:10.1007/BF00002570

Shi X, Thornton PE, Ricciuto DM, Hanson PJ, Mao J, Sebestyen SD, Griffiths NA, Bisht G (2015) Representing northern peatland microtopography and hydrology within the Community Land Model. Biogeosciences 12:6463–6477. doi:10.5194/bg-12-6463-2015

Shurpali NJ, Verma SB (1988) Micrometeorological measurements of methane flux in a Minnesota peatland during two growing seasons. Biogeochemistry 40:1–15. doi:10.1023/A:1005875307146

Shurpali NJ, Verma SB, Clement RJ (1993) Seasonal distribution of methane flux in a Minnesota peatland measured by eddy correlation. J Geophys Res 98:20649–20655. doi:10.1029/93JD02181

Song CC, Xu XF, Tian HQ, Wang YY (2009) Ecosystem-atmosphere exchange of CH_4 and N_2O and ecosystem respiration in wetlands in the Sanjiang Plain, Northeastern China. Glob Change Biol 15:692–705. doi:10.1111/j.1365-2486.2008.01821.x

Song CC, Xu XF, Sun XX, Tian HQ, Sun L, Miao Y, Wang X, Guo Y (2012) Large methane emissions upon spring thaw from natural wetlands in the northern permafrost region. Environ Res Lett 7:034009. doi:10.1088/1748-9326/7/3/034009

Tarnocai C, Stolbovoy V (2006) Chapter 2: northern peatlands: their characteristics, development and sensitivity to climate change. In: Martini LP, Martinez-Cortizas A, Chesworth W (eds) Peatlands: evolution and records of environmental and climate changes. Elsevier Science, Philadelphia, pp 17–51

Tfaily MM, Cooper WT, Kostka J, Chanton PR, Schadt CW, Hanson PJ, Iversen CM, Chanton JP (2014) Organic matter transformation in the peat column at Marcell Experimental Forest: humification and vertical stratification. J Geophys Res Biogeosci 119:661–675. doi:10.1002/2013JG002492

Tian H, Xu X, Liu M, Ren W, Zhang C, Ghen G, Lu C (2010) Spatial and temporal patterns of CH_4 and N_2O fluxes in terrestrial ecosystems of North America during 1979–2008: application of a global biogeochemistry model. Biogeosciences 7:2673–2694. doi:10.5194/bg-7-2673-2010

Venterea R, Parkin T (2012) Quantifying biases in non-steady state chamber measurements of soil-atmosphere gas exchange. In: Liebig MA, Franzluebbers AJ, Follett RF (eds) Managing agricultural greenhouse gases. Academic Press, Boston, pp 327–343

Verry ES, Brooks KN, Barten PK (1988) Streamflow response from an ombrotrophic mire. Symposium on the hydrology of wetlands in temperate and cold regions. Publications of the Academy of Finland, Helsinki, pp 52–59

Walter BP, Heimann M (2000) A process-based, climate sensitive model to derive methane emissions from natural wetlands: application to five wetland sites, sensitivity to model parameters, and climate. Glob Biogeochem Cycles 14:745–765. doi:10.1029/1999GB001204

Wania R, Ross I, Prentice IC (2010) Implementation and evaluation of a new methane model within a dynamic global vegetation model: LPJ-WHyMe v1.3.1. Geosci Model Dev 3:565–584. doi:10.5194/gmd-3-565-2010

Whiting GJ, Chanton JP (2001) Greenhouse carbon balance of wetlands: methane emission versus carbon sequestration. Tellus B 53:521–528. doi:10.1034/j.1600-0889.2001.530501.x

Zhuang Q, Melillo JM, Kicklighter DW, Prinn RG, McGuire AD, Steudler PA, Felzer BS, Hu S (2004) Methane fluxes between terrestrial ecosystems and the atmosphere at northern high latitudes during the past century: a retrospective analysis with a process-based biogeochemistry model. Glob Biogeochem Cycles 18:GB3010. doi:10.1029/2004GB002239